International Journal for Housing Science and Its Applications
Publish August 5, 2025. Volume 46, Issue 3 Pages 4365-4375

https://doi.org/10.70517/ijhsa463373

Optimization study of post-disaster resilience enhancement and resource scheduling of distribution networks in coastal cities based on mixed-integer linear programming

Guowei Liu[1], Hao Dai[1], Hao Deng[1], Lisheng Xin[1,*] and Longlong Shang[1]
[1] Distribution Network Management Department, Shenzhen Power Supply Co., Ltd., Shenzhen, Guangdong, 518000, China
Corresponding authors: (e-mail: 19928723443@163.com).

Abstract In this paper, a two-stage robust optimization model based on mixed-integer linear programming is proposed for the problem of resilience enhancement and resource scheduling optimization of distribution networks in coastal cities under extreme disasters. The optimization model of active distribution network power supply restoration is constructed to realize multi-resource cooperative scheduling by combining linearized tidal current constraints. A line maintenance team scheduling model is established to optimize the fault repair path and sequence. Design the two-stage robust optimization framework, and realize the master-slave problem iteratively solved by the column constraint generation algorithm. The simulation results show that under the three fault scenarios, the SRCL indexes of Case3 are improved by 31.108%, 39.321% and 27.42%, and the RRCL is improved by 4.355%, 19.853% and 6.703%, respectively, compared with that of Case2, and the voltage overrun problem can be effectively suppressed. The robustness analysis verifies the adaptability of the model to the uncertainty of line maintenance time, and provides decision support for the formulation of post-disaster recovery strategies.

Index Terms mixed-integer linear programming, distribution network disaster recovery, two-stage robust optimization model, column-constrained generation algorithm, grid fault repair

I. Introduction

In recent years, various extreme events have occurred frequently, especially for distribution networks, which are highly susceptible to blackouts due to various extreme natural disasters due to the fragile infrastructure and radial distribution lines [1]-[3]. In order to cope with these adverse effects, strategies and methods need to be adopted to enhance the ability of distribution networks to cope with disasters [4]. Collaborative utilization of local fixed power sources in the distribution network and mobile emergency resources to complete the restoration of the distribution network is an important means to reduce outage losses and enhance urban resilience [5]. After an extreme event, the distribution grid is disconnected from the larger grid, and multiple distribution lines are damaged, creating multiple independent electrical islands of power loss [6].

For this situation, distributed power sources in the distribution grid and dispatch emergency repairers can be coordinated to repair damaged critical paths to restore important loads, thus reducing losses [7], [8]. In this regard, during the dynamic change of the availability of damaged lines, the structure of each island in the distribution network changes accordingly, and each formed electrical island should maintain a radial topology, i.e., dynamic radial topology [9]-[11]. Based on this, a decision model based on mixed integer linear programming is proposed to ensure that post-disaster mobile resource scheduling is synchronized with distribution network load restoration, while the radial topology of the distribution network needs to be ensured in order to achieve synergistic scheduling of fixed and mobile resources [12]-[17].

In this paper, we synthesize the roles of voltage regulating equipment, microgrid, and network reconfiguration to establish an active distribution network power supply restoration model based on mixed integer linear programming model. Considering maintenance resource scheduling, a line maintenance team scheduling model is proposed. A two-stage robust optimization model is established, and the column and constraint generation algorithm is used for the co-optimization of the model. The effectiveness of the proposed model is investigated by comparing the resilience indexes of distribution networks in three scenarios under three fault conditions. The sensitivity problem of discrete robustness is analyzed to evaluate the impact of uncertainty in repair time of each type of faults on the total cost of distribution network restoration.

II. two-stage robust optimization model for distribution networks based on mixed integer linear programming

Nowadays, environmental degradation causes extreme weather events in coastal cities with high frequency, which affects the normal and stable power supply of the distribution network, causes huge economic losses, and even jeopardizes social stability. Therefore, for large-scale distribution network outages, it is necessary to develop corresponding distribution network restoration measures to improve the resilience of the distribution network to ensure the safety and stability of the distribution network.

II. A. Optimization model for active distribution network power restoration

II. A. 1) Objective function

In this paper, the objective function is constructed by minimizing the total cost of power supply restoration, which is calculated by converting the power of the disconnected loads and the number of actions of the regulating equipment uniformly into a cost. Equation (1) gives the expression of the objective function:

$$\begin{aligned}\min imize\psi = & \sum_{i\in\Omega_N^D,\Omega_{S_i}^F}\kappa_i^{LS}P_i^D\left(1-y_{S_i}^{LS}\right)+\sum_{ij\in\Omega_{SW}^R}\kappa_{ij}^{SW}\hat{\delta}_{ij}^{SW}\\ & +\sum_{i\in\Omega_N^{DG}}\left(\kappa_i^{DGp}\hat{\delta}_i^{DGp}+\kappa_i^{DGq}\hat{\delta}_i^{DGq}\right)\\ & +\sum_{i\in\Omega_N^{CB}}\kappa_i^{CB}\hat{\delta}_i^{CB}+\sum_{i\in\Omega_N^{OLTC}}\kappa_i^{OLTC}\hat{\delta}_i^{OLTC}\\ & +\sum_{ij\in\Omega_B^{VR}}\kappa_{ij}^{VR}\hat{\delta}_{ij}^{VR}+\kappa^{MG}\sum_{i\in\Omega_N^{DG+}}\lambda_i^{DG}\end{aligned} \tag{1}$$

where: i,j,n - node number; ij - branch number; Ω_N - all nodes in the system set, including the virtual substation nodes, $\Omega_N=\Omega_N^R\cup\Omega_N^F$; Ω_B - the set of all branches in the system, including virtual branches, $\Omega_B=\Omega_B^R\cup\Omega_{SW}^F$; Ω_{SW} - the set of all branched circuits with switches in the system, $\Omega_{SW}=\Omega_{SW}^R\cup\Omega_{SW}^F$; Ω_B^R - the set of actual branches; Ω_{SW}^F - set of virtual branches with switches; Ω_N^D - the set of load nodes, $\Omega_N^D=\Omega_N^R\ \ \Omega_N^{SS}$; Ω_N^{SS} - the set of actual substation nodes; Ω_N^F - the set of virtual substation nodes only; Ω_{SW}^R - the set of - the set of all actual branches with switches in the system, $\Omega_{SW}^R=\Omega_{SW}^O\ \ \Omega_{SW}^C$; $\Omega_{\mathrm{SW}}^{\mathrm{O}}$ - the actual set of branches that disconnected the switch before the fault; Ω_{SW}^C - the set of actual branches that are in the pre-failure closed switch; Ω_N^{DG} - the -the set of nodes of the DGs; Ω_N^{CB} - the set of nodes of CBs; Ω_N^{OLTC} - the set of nodes of on-load regulator transformers (OLTCs) - the set of nodes of on-load regulator transformers (OLTCs); Ω_B^{VR} - the set of branch circuits of regulators (VRs); Ω_N^{DG+} - set of nodes with DGs with black-start capacity; κ_i^{LS} - - the cost of not meeting load demand loss at node i, \$/kW; P_i^D,Q_i^D --Active/reactive power demand at node i rated voltage, kW, kVar; 0~1 variable $y_{S_i}^{LS}$ - whether the zone S_i containing node i is energized or not, $y_{S_i}^{LS}=1$ is energized, otherwise $y_{S_i}^{LS}=0$; S_i - the zone containing node i; $\kappa_{ij}^{\mathrm{SW}}$ - the cost of the branch ij switching operation, \$; $\hat{\delta}_{ij}^{\mathrm{SW}}$ -- ij branch switch operation; $\kappa_i^{\mathrm{DGp}},\kappa_i^{\mathrm{DGq}}$ - the cost of changing the active/reactive output of DG at node i, \$/kW, \$/kVar; $\hat{\delta}_i^{DGp},\hat{\delta}_i^{DGq}$ - regulation of DG active/reactive dispatch at node i, kW, kVar; κ_i^{CB} - the cost of running state of CBs at node i, \$; $\hat{\delta}_i^{CB}$ - the amount of -The amount of regulation of the number of CBs connected at node i; κ_i^{OLTC} - the cost of changing the operation of OLTC at node i, \$; $\hat{\delta}_i^{OLTC}$ - the amount of regulation of the OLTC operation at node i; κ_{ij}^{VR} - the cost of changing the VR operation at the branch ij, \$; $\hat{\delta}_{ij}^{VR}$ - the regulation of VR at branch ij, kV; κ^{MG} - the cost of forming a microgrid, in \$; 0~1 variable λ_i^{DG} - When $\lambda_i^{DG}=1$, there is at least one DG with black-start capacity operating in the microgrid containing node i.

The first term of the objective function ψ is the cost of loss of unsupplied total active load, the second term is the cost of switching operations, the third term is the cost of active and reactive dispatch regulation of the DGs, the fourth term is the cost of CBs action, the fifth and sixth terms are the cost of operation of the OLTCs and VRs, respectively, and the last term is the cost of formation of the microgrid.

II. A. 2) Linearized tidal constraints

The linearized tidal equation is:

$$\sum_{ji\in\Omega_B^n} P_{ji} - \sum_{ij\in\Omega_B^n}\left(P_{ij}+R_{ij}I_{ij}^{SQ}\right)+P_i^{SS}+P_i^{DG}=\hat{P}_i^D \tag{2}$$

$$\sum_{ji\in\Omega_B^n} Q_{ji} - \sum_{ij\in\Omega_B^n}\left(Q_{ij}+X_{ij}I_{ij}^{SQ}\right)+Q_i^{SS}+Q_i^{DG}+Q_i^{CB}=\hat{Q}_i^D,\forall i\in\Omega_N^R \tag{3}$$

$$V_i^{SQ}-V_j^{SQ}+\delta_{ij}^{VR}+\xi_{ij}=2\left(R_{ij}P_{ij}+X_{ij}Q_{ij}\right)+Z_{ij}^2I_{ij}^{SQ},\forall ij\in\Omega_B^R \tag{4}$$

$$\left|\xi_{ij}\right|\le M_{ij}\left(1-\omega_{ij}^{SW}\right),\forall ij\in\Omega_B^R \tag{5}$$

$$\vartheta_j^2 I_{ij}^{SQ}=\sum_{l=1}^{\Lambda} m_{ij,l}\left(\Delta_{ij,l}^P+\Delta_{ij,l}^Q\right),\forall ij\in\Omega_B^R \tag{6}$$

$$P_{ij}=P_{ij}^+-P_{ij}^-,\forall ij\in\Omega_B^R \tag{7}$$

$$Q_{ij}=Q_{ij}^+-Q_{ij}^-,\forall ij\in\Omega_B^R \tag{8}$$

$$P_{ij}^+ + P_{ij}^- = \sum_{l=1}^{\Lambda}\Delta_{ij,l}^P,\forall ij\in\Omega_B^R \tag{9}$$

$$Q_{ij}^+ + Q_{ij}^- = \sum_{l=1}^{\Lambda}\Delta_{ij,l}^Q,\forall ij\in\Omega_B^R \tag{10}$$

$$0\le\Delta_{ij,l}^P\le\overline{\Delta}_{ij}^s,\forall ij\in\Omega_B^R,l\in\{1,\cdots,\Lambda\} \tag{11}$$

$$0\le\Delta_{ij,l}^Q\le\overline{\Delta}_{ij}^s,\forall ij\in\Omega_B^R,l\in\{1,\cdots,\Lambda\} \tag{12}$$

where: Ω_N^R - the set of actual nodes; P_{ij},Q_{ij} - branch ij Active/reactive power, kW, kVar; R_{ij},X_{ij},Z_{ij} - resistance, impedance, impedance values of branch ij, Ω; I_{ij}^{SQ} - the square of the magnitude of the current on the branch ij, A; P_i^{SS},Q_i^{SS} - active/reactive power input to the substation at node i, kW, kVar; Q_i^{CB} - reactive power injected by CB at node i, kVar; P_i^{DC},Q_i^{DG} --Active/reactive power of the DG at node i, Kw,kVar; $\hat{P}_i^D,\hat{Q}_i^D$ - active/reactive power demanded by loads at node i, kW, kVar; V_i,V_i^{SQ} - voltage amplitude at node i and its square, kV; δ_{ij}^{VR} - VRs model with auxiliary variables ($\delta_{ij}^{VR}=0$ for branches without VR); ξ_{ij} - the slack variable in the calculation of the branch voltage drop ($\xi_{ij}=0$ for the unswitched branch); M_{ij} - the calculation of the ij branch voltage Big-M value of the drop; ω_{ij}^{SW} - whether the branch ij switch is on or not, $\omega_{ij}^{SW}=0$ means it is on, otherwise $\omega_{ij}^{SW}=1$. For branches without switches, $\omega_{ij}^{SW}=1$; ϑ_i - pre-fault estimation of voltage amplitude at node i, Kv; A - number of segments for segment linearization; l -- index of the linearized segment; $m_{ij,l}$ - the slope of the segment linearized segment 1 on branch ij; $\Delta_{ij,}^P,\Delta_{ij\mu}^0$ - the discrete variable associated with segment 1 for active/reactive currents on branch ij; P_{ij}^+,P_{ij}^- - the non-negative variable for active power on branch ij, kW; Q_{ij}^+,Q_{ij}^- - non-negative variable of reactive power on branch ij, kVar; $\overline{\Delta}_{ij}^s$ - length of each segment linearized to the square of power on branch ij.

Constraints Eqs. (2) and (3) represent the Kirchhoff current constraints, and these equations include the active and reactive power injected by the DGs and the reactive power injected by the CBs. Constraint Eq. (4) represents the Kirchhoff voltage constraint, and the slack variable ξ_{ij} in Eq. (4) is computed based on ω_{ij}^{sw} in Eq. (5), and $M_{ij}=\left(\overline{V}^2-\underline{V}^2\right)$ for the branch without VR; For branches with VR, $M_{ij}=\left(\overline{V}^2-\underline{V}^2\right)+\overline{\Delta}_{ij}^{VR}\left(2+\overline{\Delta}_{ij}^{VR}\right)\overline{V}^2$. If $\omega_{ij}^{SW}=1$, then $\xi_{ij}=0$; if $\omega_{ij}^{SW}=0$, the squared values of the voltage magnitudes in Eq. (4) are independent. Finally, the segmented

linearization Eqs. (6) to (12) provides the branch I_{ij}^{se}, where the length of each segment of the trend-squared linearization is $\overline{\Delta}_{ij}^{s} = \overline{VI}_{ij} / \Lambda$, and the slope of each segment is $m_{i,j,1} = (5/6)\overline{\Delta}_{ij}^{s}$ and $m_{ij,} = (2l-1)\overline{\Delta}_{ij}^{s}$, where $l > 1$.

II. B.Line Maintenance Fleet Scheduling Model

Line maintenance teams, as an important disaster recovery resource, can reduce the outage time by modeling them rationally, optimizing the scheduling of line maintenance teams, and solving for reasonable repair paths and repair sequences. The line maintenance team scheduling model is an important part of the disaster recovery model by deciding the line maintenance team path to repair the faulty line. The line maintenance team scheduling model consists of two parts, the line maintenance team scheduling path model and the line maintenance team scheduling time model.

Line maintenance team scheduling path model: the line maintenance team receives the instruction to start the post-disaster recovery work, the first from the maintenance site, after the planned maintenance path, maintenance of the corresponding fault line, after completion of the final return to the original maintenance site, on the way is not allowed to move to other maintenance sites. First of all, a maintenance team to leave the maintenance site and finally return to the same maintenance site for modeling, model constraints as shown in equation (13):

$$\begin{cases} \sum\limits_{k} x_{dp(mc),k,mc}^{MC} = \sum\limits_{k} x_{k,dp(mc),mc}^{MC} = 1, \forall mc \\ \sum\limits_{k} x_{dp,k,mc}^{MC} = \sum\limits_{k} x_{k,dp,mc}^{MC} = 0, \forall mc, \forall dp \in DP / \{dp(mc)\} \end{cases} \tag{13}$$

where $x_{k,l,mc}^{MC}$ is a line maintenance team scheduling variable that indicates whether a certain line maintenance team mc is scheduled from faulty node k to faulty node l. If $x_{k,l,mc}^{MC} = 1$ it means that line maintenance team mc is dispatched from faulty node k to faulty node l, and if $x_{k,l,mc}^{MC} = 0$ it means that line maintenance team mc is not dispatched from faulty node k to faulty node l. The nodes in $x_{k,l,mc}^{MC}$ are not line nodes, but nodes on the movement path of the line repair team, including the repair site and the location of the faulted line, where dp denotes the repair team site, k and l denote the faulted line, mc denotes the line repair team, DP denotes the collection of the repair team sites, and $DP / \{dp(mc)\}$ denotes the set of repair sites other than its own.

After a line repair team mc arrives at fault node k, it will first repair the line fault at that node, and after repairing the fault is completed, the team will arrive at another fault node l to repair another line fault, and the team will not repeatedly pass through the same fault node, whose model constraints are shown in Eq. (14):

$$\sum_{l} x_{k,l,mc}^{MC} = \sum_{l} x_{l,k,mc}^{MC} \le 1, \forall mc, \forall k \in V^{MC} / DP \tag{14}$$

where V^{MC} denotes the set of faulty nodes and repair team sites, V^{MC} / DP denotes the set of faulty nodes, and "≤ 1" instead of "$= 1$" is because it is not necessary for a certain repair team to repair all the faulty nodes, but rather requires multiple repair teams to coordinate their scheduling to repair all faults.

The scheduling instruction stipulates that each faulty line only appears in the scheduling path of one line maintenance team, i.e., each faulty line requires only one line maintenance team to repair it without the participation of other line maintenance teams, which avoids the waste of maintenance resources, and at the same time accelerates the process of repairing faults to increase the recovery of power supply. The model constraints are shown in equation (15):

$$\sum_{mc} \sum_{l} x_{l,k,mc}^{MC} = 1, \forall k \in V^{MC} / DP \tag{15}$$

The scheduling time model of the line maintenance team: the line maintenance team arrives at a faulty line at a certain moment, carries out maintenance work for a certain period of time, and rushes to the next faulty line after a period of time after the completion of the repair, and so on and so forth until the fault is completely repaired. Set the moment when a line repair team mc arrives at a faulty node k as $A_{k,mc}^{MC,AR}$; the repair time of the faulty node k is set to $T_{k,mc}^{RP}$ and assume that any repair team spends the same amount of time repairing the same fault; set the moment when the repair of the faulty node k finishes as $A_{k}^{MC,RP}$; set the time taken by the line repair team mc to move from fault node k to fault node l to be $T_{k,l,mc}^{TR}$; and set the moment when the line repair team mc

reaches fault node l from fault node k to be $A_{l,mc}^{MC,AR}$. From this, we can get the expression of the time relationship between the line maintenance team from arriving at fault node k, after repairing the fault, moving to fault l, as shown in equation (16):

$$A_{l,mc}^{MC,AR} = A_{k,mc}^{MC,AR} + T_{k,mc}^{RP} + T_{k,l,mc}^{TR} \tag{16}$$

At this time, the line maintenance team scheduling variable $x_{k,l,mc}^{MC} = 1$, however, the scheduling path is not necessarily in the order of fault node k to fault node l, so in order to perform a global unified modeling, the moment when the maintenance team reaches fault node l must be constrained by the line maintenance team scheduling variable $x_{k,l,mc}^{MC}$, which loosely transforms Eq. (16) into Eq. (17), i.e:

$$\begin{cases} A_{l,mc}^{MC,AR} \le A_{k,mc}^{MC,AR} + T_{k,mc}^{RP} + T_{k,l,mc}^{TR} + \left(1 - x_{k,l,mc}^{MC}\right) \\ \cdot M, \forall mc, \forall k, l \in V^{MC} \\ A_{l,mc}^{MC,AR} \ge A_{k,mc}^{MC,AR} + T_{k,mc}^{RP} + T_{k,l,mc}^{TR} - \left(1 - x_{k,l,mc}^{MC}\right) \\ \cdot M, \forall mc, \forall k, l \in V^{MC} \end{cases} \tag{17}$$

where M denotes an extremely large constant. The inequality constraint (17) defines the upper and lower bounds of $A_{l,mc}^{MC,AR}$, which determines the moment when the line repair team mc arrives at the faulted node, and the next step needs to be a reasonable modeling of the moment when the line repair team mc repairs the completed fault $A_k^{MC,RP}$ as shown in equation (18):

$$A_k^{MC,RP} = \sum_{mc} \left(A_{k,mc}^{MC,AR} + T_{k,mc}^{RP} \cdot \sum_{l} x_{l,k,mc}^{MC} \right), \forall k \in V^{MC} \tag{18}$$

where $A_k^{MC,RP}$ denotes the moment when the repair is completed at node k, any line repair team repairs fault node k, then the moment when fault k is repaired can be determined by the expression. Eq. (18) determines the moment when the line repair team reaches the latter fault node l, and then it is necessary to model the moment when the line repair team reaches the fault node k, if the scheduling instructions do not schedule a line repair team to reach the fault node k, then its corresponding line repair team reaches the moment when the fault node k $A_{k,mc}^{MC,AR}$ is 0, as shown in equation (19).

$$0 \le A_{k,mc}^{MC,AR} \le M \cdot \sum_{l} x_{l,k,mc}^{MC}, \forall mc, \forall k \in V^{MC} \tag{19}$$

II. C. Two-stage robust optimization model construction and solution

The distribution network quantifies the impact of equipment at each node on the system resilience under extreme weather conditions and allocates standby power at key nodes to improve the system resilience, and proposes a multi-objective optimization model to determine the location and capacity of the gas-fired unit, which turns the optimization of the system resilience into the optimization of the economic cost. A two-stage robust optimization (RO) model is established to comprehensively consider the resilience improvement of the grid system.

In order to seek to achieve the shortest fault repair time under the worst conditions, the following model is established:

$$\begin{cases} \min\limits_{X} \max\limits_{u} \min\limits_{Y} \sum\limits_{d=1}^{D} \sum\limits_{r \in R_d} \tau_{r,d} \\ X = [P_{g,t}, Q_{g,t}, P_{ij,t}, Q_{ij,t}, \alpha] \\ u = [T_{b,i,j}(t)] \\ Y = [\tau_{r,d}] \end{cases} \tag{20}$$

where: $\tau_{r,d}$ is the time required by the overhaul team d to repair the faulty line element r, D is the number of overhaul teams, and R_d is the set of faulty elements.

The stage 1 decision vector is X, with the objective of system hardware reinforcement to minimize the configuration cost, and the stage 2 decision vector is Y, with the objective of minimizing the amount of load shedding and uncertainty variables, in order to seek the fastest restoration of the faulty components under the worst path.

Considering the amount of load shedding and the number of configured contact switches, the following constraint model for minimizing the cost of both is developed:

$$f = \min_{Y} \sum_{t=1}^{T} \sum_{j \in S_h} c_1 P^{L,Shd} + \sum_{t=1}^{T} \sum_{i,j \in S_{tie}} c_2 a_{ij,t} \tag{21}$$

where c_1 is the unit cost of load abandonment, c_2 is the unit investment cost of contact switch, S_{lc} is the set of lines, and T is the total operating time.

Eqs. (20) and (21) portray the maintenance travel time uncertainty model and the distribution network short-time reconfiguration optimization model, respectively, and the 2 models can be solved conjointly by establishing the coupling relationship between the faulty element state and the restoration state, i.e., the integrated model:

$$F = \min \left(\sum_{t=1}^{T} \sum_{j \in S_{lc}} c_1 P_{l,shd} + \sum_{t=1}^{T} \sum_{i,j \in S_{lc}} c_2 a_{i,j,t} + \max_u \min \sum_{d=1}^{D} \sum_{r \in R_d} c_3 \tau_{r,d} \right) \tag{22}$$

where: c_3 is the unit time cost of fault repair.

The model is decomposed into the master problem (MP) and subproblems (SP), and iterated repeatedly to obtain the optimal solution: the MP minimizes part of the problem and relaxes part of the constraints, thus providing a lower bound on the optimal value, while the SP maximizes part of the problem to provide a feasible solution to the original problem, which can be used as an upper bound on the optimal solution. The master problem and subproblems are continuously updated and converged to obtain the optimal solution.

The MP form is as follows:

$$\begin{cases} \min_X \eta \\ s.t.\ AX \le b \\ \eta \ge q^T Y_l, \quad l \le K \\ BX + CY_l \le g - Eu_l^-, \quad l \le K \end{cases} \tag{23}$$

where q, b and g are constant matrices, A, B, C and E are constant coefficient matrices, η is an auxiliary variable, u_l^- is the worst-case travel scenario for the l th iteration, Y_l is the auxiliary matrix added to the main problem for the l th iteration, and K is the maximum number of iteration number of iterations.

The SP form is as follows:

$$\begin{cases} \max_u \min_Y q^T Y_l \\ s.t.\ CY \le g - BX^* - Eu_l^- \end{cases} \tag{24}$$

where X^* is the optimal solution to the master problem.

The subproblem (24) is transformed into the following single-level optimization problem according to the dyadic theory:

$$\begin{cases} \max_{\tilde{u},\lambda} (g - BX - E\tilde{u})^T \lambda \\ s.t.\ C^T \lambda = q \\ \lambda \le 0 \end{cases} \tag{25}$$

For $(E\tilde{u})^T \lambda$, an auxiliary variable μ is introduced with the same dimension as $\tilde{u}$ as follows:

$$\tilde{u} = u_{\min} + (u_{\max} - u_{\min}) \mu \tag{26}$$

where $u_{\max}$ is the worst value of the scene and $u_{\min}$ is the best value of the scene.

This bilinear term can be transformed into:

$$\tilde{u}^T E^T \lambda = [(u_{\max} - u_{\min})\mu]^T E^T \lambda + u_{\min}{}^T E^T \lambda \tag{27}$$

A matrix H of variables of the same dimension as E is introduced and linearized using the large M method:

$$\begin{cases} -M\mu_n \le H_{mn} \le M\mu_n \\ \lambda_m E_{mn} - M(1-\mu_n) \le H_{mn} \le \lambda_m E_{mn} + M(1-\mu_n) \end{cases} \tag{28}$$

The main and subproblems are solved iteratively by the Column and Constraint Generation (C&CG) algorithm, the algorithm flow is shown in Fig. 1.

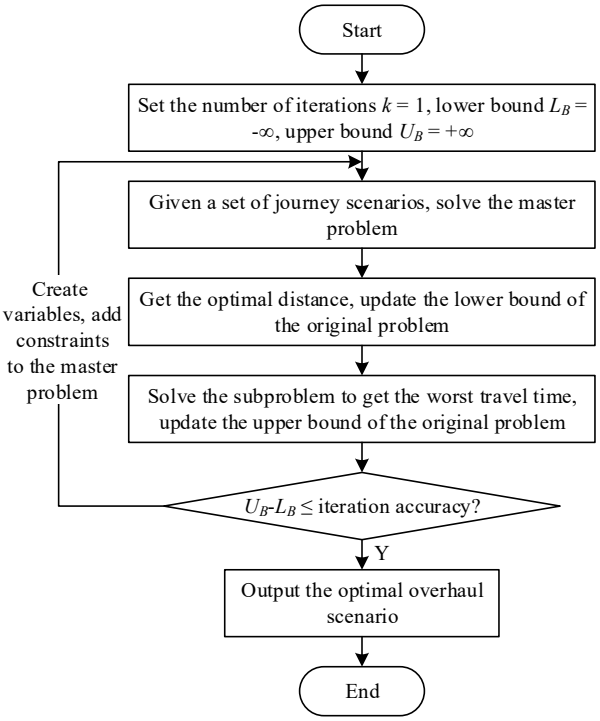

Figure 1: Two stage robust optimization solution process

III. Simulation Analysis of Post-Disaster Resilience Enhancement and Resource Dispatch Optimization of Distribution Grid in Coastal Cities

III. A. Test System and Simulation Scenario Setting

In this paper, a nodal distribution network is selected as the test simulation system, which is equipped with 4 line contact switches, 51 line sectional switches, 8 nodes as critical load nodes, and the distribution network contains 3 MGs. In order to describe the simulation results in a more understandable way, energy storage is selected as a typical flexibility resource. Voltage measurement devices are installed at nodes 5, 8, 16, 25, and 31, and the measurement devices sample data every 15 minutes to obtain operating voltage data, and nodes 4, 7, and 15 are used as flexibility resource nodes.

In this paper, the following three simulation scenarios are set up:

Case1: This test scenario adopts the optimization model of distribution network power supply restoration to cope with three typical extreme disaster fault scenarios and enhance the post-disaster resilience of the distribution network, and does not consider the scheduling of line maintenance teams;

Case2: This test scenario considers two phases of distribution network power supply restoration and line maintenance team scheduling to improve distribution network resilience, but does not consider two-phase robust optimization;

Case3: The test scenario is the resilience of distribution networks in response to three typical extreme disaster scenarios with the RO model constructed in this paper.

III. B. Analysis of distribution network resilience improvement results

III. B. 1) RO model parameterization

The PV output curves and load fluctuation curves for four typical days of spring, summer, fall and winter throughout the year are derived from the actual data of the distribution network of a coastal city, and the PV output curves are shown in Fig. 2 and the load fluctuation curves are shown in Fig. 3. Combining Fig. 2 and Fig. 3, it can be seen that both PV output and load fluctuation are the largest in summer.

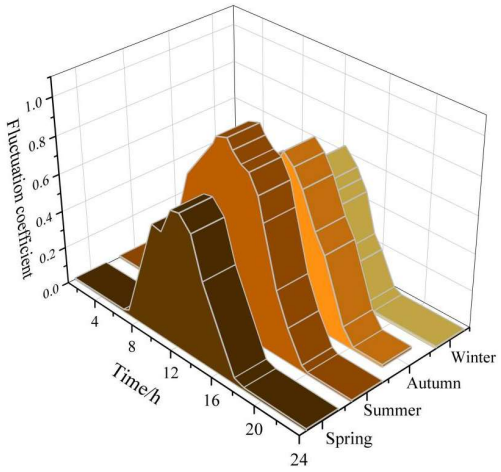

Figure 2: Output curves of photovoltaic power in four seasons

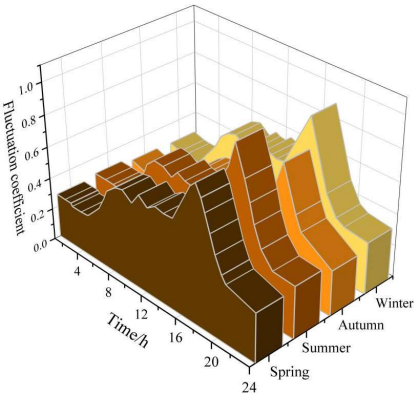

Figure 3: Seasonal load fluctuation curves

III. B. 2) Algorithm effectiveness analysis

Applying the RO model proposed in this paper to cope with three typical fault scenarios under extreme disasters, the comparison results of the survivability and resilience indicators of the distribution network under the three scenarios are shown in Table 1.

The comparison results of the resilience indexes of the distribution network under the three fault scenarios in the three scenarios show that, for the load resilience indexes SRL and RRL enhancement, Case3 does not have an obvious advantage over Case1 and Case2, and the biggest SRL enhancement of Case3 over Case2 is in the Fault1 fault scenario, with an enhancement of 1.392%, and the biggest RRL enhancement is in the Fault2 Fault2 fault scenario with the largest RRL improvement of 8.569%. However, in terms of SRCL and RRCL enhancement of critical load resilience metrics in distribution networks, the enhancement effect of Case3 has a great advantage. Under the three fault scenarios, the SRCL metrics of Case3 are improved by 31.108%, 39.321%, and 27.42%, and the RRCL is improved by 4.355%, 19.853%, and 6.703%, respectively, compared with Case2, and the RRCL metrics of Case3 under the three fault scenarios are more than 90%, which means that, during the continuation of the disaster and its recovery, the 90% of the critical load is recovered. The above analysis results show that the RO model proposed in this paper effectively improves the survival and recovery rates of distribution network critical loads under extreme disasters, and the resilience of the distribution network is significantly improved.

Table 1: Comparison Results of Distribution Network Indicators (%)

	Fault1				Fault2			
	SRL	SRCL	RRL	RRCL	SRL	SRCL	RRL	RRCL
Case1	30.407	37.376	95.645	95.645	47.596	17.805	54.440	79.949
Case2	32.036	37.376	98.756	95.645	50.362	17.964	90.413	79.949
Case3	33.428	68.484	99.848	100.000	51.618	57.285	98.982	99.802
	Fault3							
	SRL	SRCL	RRL	RRCL				
Case1	29.661	29.683	79.129	86.227				
Case2	30.288	30.023	81.618	86.425				
Case3	31.408	57.443	88.942	93.128				

III. B. 3) Resilience enhancement results

When the optimal scheduling of energy storage is not performed, the flexibility resource node has a high voltage and crosses the upper limit due to the PV output, and at the same time, there is a low voltage and crosses the lower limit due to the customer's high electric load and the PV output is 0. Under the Case3 scenario, the scheduling strategy under the case of the maximum value of the calculated energy storage is selected as the optimal strategy, and the nodes 4 and 7 are respectively combined with the node 15 to optimize the charging and discharging curves of the energy storage, as shown in Figure 4, where the storage output below the zero axis represents that the energy storage is in the charging state. 4, where the energy storage output below the zero axis represents that the energy storage is in charging state, and the energy storage output above the zero axis represents that the energy storage is in discharging state. After the optimization of RO model, its node voltage situation is obviously improved, which effectively solves the voltage overrun problem of the distribution network.

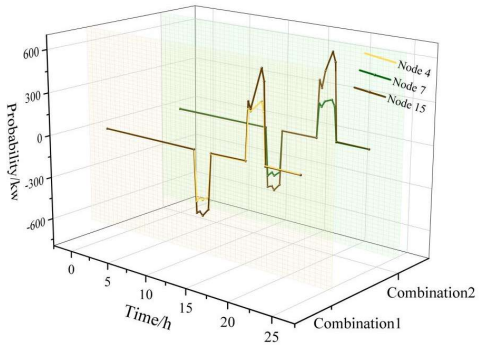

Figure 4: Charge and discharge curves for energy storage optimization

Using the RO model optimization, the generation dispatch and load restoration of each island of the distribution network after the disaster is shown in Fig. 5. As can be seen in Fig. 5, the RO model transfers the power from silos 2 and 3 to silo 1 to equalize the generation resources of each silo. At the same time, in the time domain, it presents fixed energy storage characteristics, in island 1, charging when the generation resources are rich, discharging when the generation resources are lacking, playing the role of “peak shaving and valley filling”.

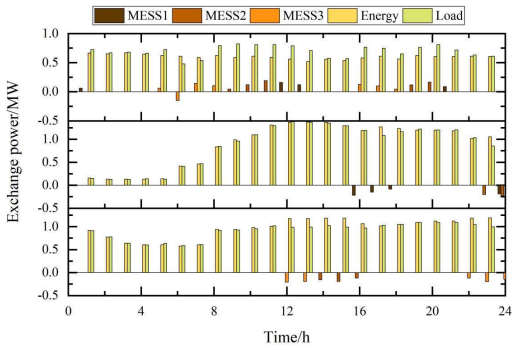

Figure 5: Power generation dispatching and load recovery situation

III. C. Fault Repair Time Uncertainty Analysis

In this section, we focus on the sensitivity of discrete robustness, and use the enumeration method to analyze the impact of robust parameters of line maintenance time uncertainty on the total system cost. All the robust parameter combinations are listed and simulated, and the simulation results are shown in Table 2 (the base for the calculation of the “percentage increase” in the table is the simulation results of the three typical failure scenarios in which the repair time is determined).

Table 2 shows that the total system cost in the simulation results of No. 1 and No. 4 are the same, both are 92.86 million yuan, which indicates that the uncertainty of the repair time of the Fault3 fault has a negligible effect on the total system cost. In addition, from the simulation results of No. 2 and No. 3, it can be seen that the degree of impact of Fault1 is higher than that of Fault2, with an increase percentage of 1.13% and 1.07%, respectively. This is of guiding significance for the development of maintenance plans for post-disaster distribution networks, which can focus on fault location and identification of the faulted lines of Fault1 and Fault2 in order to reduce the uncertainty of their maintenance time, and then develop a more reasonable maintenance plan to reduce the economic losses of post-disaster distribution networks.

Table 2: Robust analysis simulation results

Number	Line robust parameters			Total cost/ten thousand yuan	Growth percentage/%
	Fault1	Fault2	Fault3		
1	0	0	0	9.286	0.00
2	1	0	0	9.391	1.13
3	0	1	0	9.385	1.07
4	0	0	1	9.286	0.00
5	1	1	0	9.462	1.90
6	1	0	1	9.391	1.13
7	0	1	1	9.385	1.07
8	1	1	1	9.462	1.90

IV. Conclusion

In this paper, a two-stage robust optimization model for distribution networks based on mixed integer linear programming is constructed, and three simulation scenarios are set up to explore the effectiveness of the proposed RO model.

For the load resilience indexes SRL and RRL enhancement, Case3 does not have obvious advantages over Case1 and Case2, and the largest SRL enhancement of Case3 over Case2 is for the Fault1 fault case, with an enhancement of 1.392%, and the largest RRL enhancement is for the Fault2 fault case, with an enhancement of 8.569%. However, in terms of SRCL and RRCL enhancement of critical load resilience metrics of the distribution network, the enhancement of Case3 has a great advantage. Under the three fault scenarios, the SRCL metrics of Case3 are improved by 31.108%, 39.321%, and 27.42%, and the RRCL is improved by 4.355%, 19.853%, and 6.703%, respectively, compared with Case2, and the RRCL metrics of Case3 are over 90% under all three fault scenarios.

Under Case3 scenario, the voltage situation of flexibility resource nodes is significantly improved after optimization by RO model. The RO model transfers the power from silos 2 and 3 to silo 1 in order to balance the generation resources of each silo. At the same time, in the time domain, it shows the fixed energy storage characteristics, in island 1, charging when the generation resources are rich, and discharging when the generation resources are deficient, which plays the role of “peak shaving and valley filling”.

Robust analysis simulation results show that the maintenance time uncertainty of Fault3 has a negligible impact on the total system cost, and the impact of Fault1 is higher than that of Fault2, with an increase of 1.13% and 1.07%, respectively. It is further verified that the robust optimization method can effectively assess the impact of the repair time uncertainty of each type of faults on the total cost of distribution network restoration, which is a guidance for the development of the maintenance plan of the distribution network after the disaster.

Funding

This research was supported by the Science and Technology Project of China Southern Power Grid Company Limited (Project No. 090000KKK52222158).

References

[1] Zio, E., & Duffey, R. B. (2021). The risk of the electrical power grid due to natural hazards and recovery challenge following disasters and record floods: What next?. In Climate change and extreme events (pp. 215-238). Elsevier.

[2] Wang, Y., Chen, C., Wang, J., & Baldick, R. (2015). Research on resilience of power systems under natural disasters—A review. IEEE Transactions on power systems, 31(2), 1604-1613.

[3] Fang, Y. P., Sansavini, G., & Zio, E. (2019). An optimization‐based framework for the identification of vulnerabilities in electric power grids exposed to natural hazards. Risk Analysis, 39(9), 1949-1969.

[4] Ali, G. G., El-adaway, I. H., Sims, C., Holladay, J. S., & Chen, C. F. (2023). Reducing the vulnerability of electric power infrastructure against natural disasters by promoting distributed generation. Natural Hazards Review, 24(2), 04022052.

[5] Tan, Y., Qiu, F., Das, A. K., Kirschen, D. S., Arabshahi, P., & Wang, J. (2019). Scheduling post-disaster repairs in electricity distribution networks. IEEE Transactions on Power Systems, 34(4), 2611-2621.

[6] Hou, H., Tang, J., Zhang, Z., Wu, X., Wei, R., Wang, L., & He, H. (2023). Stochastic pre‐disaster planning and post‐disaster restoration to enhance distribution system resilience during typhoons. Energy Conversion and Economics, 4(5), 346-363.

[7] Shi, Q., Wan, H., Liu, W., Han, H., Wang, Z., & Li, F. (2023). Preventive allocation and post-disaster cooperative dispatch of emergency mobile resources for improved distribution system resilience. International Journal of Electrical Power & Energy Systems, 152, 109238.

[8] Lei, S., Chen, C., Li, Y., & Hou, Y. (2019). Resilient disaster recovery logistics of distribution systems: Co-optimize service restoration with repair crew and mobile power source dispatch. IEEE Transactions on Smart Grid, 10(6), 6187-6202.

[9] Gazijahani, F. S., Salehi, J., & Shafie-Khah, M. (2022). Benefiting from energy-hub flexibilities to reinforce distribution system resilience: A pre-and post-disaster management model. IEEE Systems Journal, 16(2), 3381-3390.

[10] Wan, H., Liu, W., Zhang, S., Qie, D., Shi, Q., & Cheng, R. (2025). Pre-disaster allocation and post-disaster dispatch strategies of power emergency resources for resilience enhancement of distribution networks. Electric Power Systems Research, 238, 111038.

[11] Wu, H., Xie, Y., Xu, Y., Wu, Q., Yu, C., & Sun, J. (2022). Robust coordination of repair and dispatch resources for post-disaster service restoration of the distribution system. International Journal of Electrical Power & Energy Systems, 136, 107611.

[12] Shen, Y., Qian, T., Li, W., Zhao, W., Tang, W., Chen, X., & Yu, Z. (2023). Mobile energy storage systems with spatial–temporal flexibility for post-disaster recovery of power distribution systems: A bilevel optimization approach. Energy, 282, 128300.

[13] Chen, L., Li, Y., Chen, Y., Liu, N., Li, C., & Zhang, H. (2022). Emergency resources scheduling in distribution system: From cyber-physical-social system perspective. Electric Power Systems Research, 210, 108114.

[14] Qin, C., Lu, J., Zeng, Y., Liu, J., Wu, G., & Chen, H. (2024). Optimal two-stage dispatch method of distribution network emergency resources under extreme weather disasters. Sustainable Energy, Grids and Networks, 38, 101321.

[15] H. Li H, Y.X. Zhang, Y , S.J. Guo, et al. A comprehensive study on texture evolution and recrystallisation behaviour of Fe-50Co alloy, Electrical Materials and Applications, 1 (1) e12010, 2024.

[16] H. Sun, Y.L. Shang, Y. Han, et al. Research on magnetic field characteristics of amorphous alloy and grain-oriented silicon steel hybrid magnetic circuit iron core, Electrical Materials and Applications, 1 (2) e12014, 2024.

[17] X.Y. Wang, R.F. Xue, G Ma. Error analysis and correction strategy for measuring oriented silicon steel by SST method, 1 (2) e70002, 2024.